Titan's Ionic Species: Theoretical Treatment of N_2H^+ and Related Ions†

V. Brites and M. Hochlaf*

Université Paris-Est, Laboratoire Modélisation et Simulation Multi Echelle, MSME FRE 3160 CNRS, 5 bd Descartes, 77454 Marne-la-Vallée, France

Received: April 22, 2009; Revised Manuscript Received: May 29, 2009

We use different *ab initio* methods to compute the three-dimensional potential energy surface (3D-PES) of the ground state of N_2H^+. This includes the standard coupled cluster, the complete active space self-consistent field, the internally contacted multi reference configuration interaction, and the newly developed CCSD(T)-F12 methods. For the description of H and N atoms, several basis sets are tested. Then, we incorporate the 3D-PES analytical representations into variational calculations of the rovibrational spectrum of $N_2H^+(\tilde{X}^1\Sigma^+)$ up to 7200 cm^{-1} above the zero point vibrational energy. Our data show that the CCSD(T)-F12/aug-cc-pVTZ approach represents a compromise for good description of the PES and computation cost. This technique is recommended for full dimensional PES generation of atmospheric and astrophysical relevant polyatomic systems. We applied this method to derive the rovibrational spectra of $N_2H^+(\tilde{X}^1\Sigma^+)$ and of $N_2H^{++}(\tilde{X}^2\Sigma^+)$. Finally, we discuss the existence of the $N_2H^{++}(\tilde{X}^2\Sigma^+)$ in Titan's atmosphere.

I. Introduction

N_2H^+ ion is definitely detected in the ionosphere of Titan. In 1996, Fox and Yelle[1] located a domain where N_2H^+ dominates through modeling the complex chemistry of this ionosphere. They gave the major production and loss sources of this cation depending on the altitude. They showed that this ion is produced mainly via ion−molecule reactions involving the N_2^+, H_3^+, NH^+, H_2^+, N_2 and H_2 species. These authors showed that the N_2H^+ ion reactions with neutral Titan's hydrocarbons together with dissociative recombination processes are the major routes for the decomposition of this singly charged ion. More recently, Vuitton et al.[2] confirmed these observations in close agreement with the Cassini spacecraft measurements. N_2H^+ is also of astrophysical importance. It is a selective tracer of quiescent and ionized gases in interstellar media.[3−8]

Because of its importance for astrochemistry and atmospheric chemistry, N_2H^+ was widely studied both experimentally and theoretically. Recently, Špirko, Bludský and Kraemer[9] reviewed the literature on this cation. In the following, we present only the most accurate and recent works that we will use below for the validation of our *ab initio* data. Briefly, the analysis of the velocity-modulated IR laser spectra of Saykally and co-workers[10,11] and the tunable diode laser IR spectrum of Foster and McKellar[12] allowed the determination of the fundamentals and the vibration−rotation terms of $N_2H^+(\tilde{X}^1\Sigma^+)$. Later on, the full spectrum of the fundamentals, overtones and combination modes of $N_2H^+(\tilde{X}^1\Sigma^+)$ up to ∼10 600 cm^{-1} is determined through the analysis of Kabbadj et al.'s highly resolved IR spectrum.[13] For the rotational constants and equilibrium geometry determinations, we will refer to the submillimeter-wave spectroscopy work by Amano, Hirao and Takano.[14] Theoretically, the potential energy surface and the rovibrational spectrum of $N_2H^+(\tilde{X}^1\Sigma^+)$ were generated using the basis sets and the methods implemented in the computational packages before 2000. These techniques and the corresponding results are also discussed in ref 9. For N_2D^+, a full set of accurate data is available.[12,15,16] Therefore, N_2H^+ and its deuterated species represent benchmark ionic polyatomic molecular systems for checking the accuracy of *ab initio* techniques and methodologies devoted for studying atmospheric and astrophysical relevant molecules.

In reactive and nonreactive collisional and dynamical calculations, one needs a huge number of energies for different nuclear configurations for the generation of full dimensional potential energy surfaces. These calculations are mandatory for the modeling of the reactions involving astrophysical and atmospheric relevant systems and for the determination of their rates. The standard methods are computationally time consuming. Taking advantage of the new developments, we would like to establish an accurate enough methodology with low computation cost for that purpose. Therefore, we map here the three-dimensional potential energy surface (3D-PES) of the ground state of N_2H^+ ion using multiconfigurational and monoconfigurational approaches in connection with different basis sets. Then, we check the accuracy of the spectroscopic data and the rovibrational spectra by direct comparison with the experimental results. Recently, we proved that the N_2H^{++} dication is bound.[17] We predict a full set of spectroscopic constants for N_2H^{++} $\tilde{X}$ and its rovibrational spectrum. Finally, we discuss the implications of the presence of N_2H^{++} in the atmosphere of Titan.

II. Theoretical Methods

a. Electronic Structure Calculations. We performed electronic computations using several methodologies: (i) multi configurational approaches such as complete active space self-consistent field (CASSCF),[18] followed by the internally contracted multireference configuration interaction (MRCI) method[19,20] with and without the inclusion of the Davidson correction for quadruple excitations;[21] (ii) mono configurational methods including coupled cluster approach without (CCSD) and with perturbative treatment of triple excitations (CCSD(T)).[22] For coupled cluster computations, we used the standard methods as implemented in MOLPRO.[23] We also used the newly developed and implemented (R)CCSD(T)-F12 technique (both F12a and F12b approximations)[24,25] as described in refs 23 and

† Part of the special section "Chemistry: Titan Atmosphere".

* To whom correspondence should be addressed. E-mail: hochlaf@univ-mlv.fr.

10.1021/jp903701x CCC: $40.75
Published on Web 06/25/2009

TABLE 1: Total CPU Time (in Seconds), Disk Used, Number of Gaussian Functions (GTOs) and Number of Configuration State Functions (CSFs) for a Single Point Calculation on the $\tilde{X}^1\Sigma^+$ Electronic Ground State of N_2H^+ in the C_{2v} Point Group[a]

method	GTOs	CSFs	disk used	total CPU time[b]
CASSCF/aug-cc-pV6Z	505	1436	25.35 GB	7125.38
MRCI/aug-cc-pV6Z	505	39.3×10^7	25.35 GB	8594.32
CCSD(T)/cc-pV5Z	237	172344	1.31 GB	178.13
CCSD(T)/cc-pV5Z-DK	237	172344	1.31 GB	185.14
CCSD(T)/aug-cc-pV5Z	334	346204	5.03 GB	1042.99
CCSD(T)/aug-cc-pV6Z	505	796078	25.35 GB	8000.58
CCSD(T)-F12/aug-cc-pVDZ	55	8140	41.15 MB	4.66
CCSD(T)-F12/aug-cc-pVTZ	115	39211	120.20 MB	23.82
CCSD(T)-F12/aug-cc-pVQZ	206	129984	839.61 MB	158.07
CCSD(T)-F12/aug-cc-pV5Z	334	346204	5.03 GB	1295.98

[a] Internal coordinates are set to $R_{NN} = 2.05$ bohr, $R_{NH} = 1.95$ bohr and in-plane angle $\theta = 180°$. These computations are performed in a X5460@3.16 GHz processor and using the 2008.1 version of MOLPRO.[23] [b] Total CPU time is for a total energy evaluation.

26. Briefly, the CCSD-F12 calculations start by DF-MP2-F12/3C(FIX) calculations. Then, the CCSD-F12 computations are performed without density fitting. During the DF-MP2 calculations a density fitting is done. Finally, the triples correction is included to the CCSD-F12 energies.

The electronic calculations start with HF computations on the electronic ground state of $N_2H^+(\tilde{X}^1\Sigma^+)$ to reduce symmetry-breaking problems. In CASSCF, the active space includes all valence electrons and all valence orbitals. In MRCI, all configurations of the CI expansion of the CASSCF wave functions are taken into account as a reference. The numbers of configuration state functions (CSFs) for the A_1 symmetry of the C_{2v} point group are specified in Table 1.

We considered several basis sets for the description of nitrogen and hydrogen atoms. For CASSCF, MRCI and (R)CCSD(T) calculations, we employed the Dunning and coworkers basis sets, such as cc-pV5Z, cc-pV5Z-DK, aug-cc-pV5Z, aug-cc-pV6Z.[27−29] In (R)CCSD(T)-F12 computations, the aug-cc-pVXZ (X = D, T, Q and 5) in connection with the corresponding auxiliary basis sets and density fitting functions, which are needed for CCSD(T)-F12 method, are used. This is described in refs 30−32. Table 1 gives the number of contracted Gaussian functions (GTOs) considered in each calculation.

We did all electronic calculations with the MOLPRO program suite[23] in C_{2v} or C_s point groups. Table 1 lists the computational time and the disk occupation for a $N_2H^+(\tilde{X}^1\Sigma^+)$ single point computation, that is, by considering the A_1 symmetry in the C_{2v} point group.

b. Analytical Representation of the 3D-PESs. We generated the 3D-PESs in the internal coordinates. They comprise the two stretching coordinates R_1 (R_{NN}), R_2 (R_{NH}) and the in-plane bending angle θ (NNH). We calculated energies corresponding to different nuclear positions in the vicinity of the equilibrium geometry of $N_2H^+(\tilde{X}^1\Sigma^+)$. We considered geometries in the ranges (in Å and degrees) $1.8 \le R_1 \le 2.65$, $1.75 \le R_2 \le 2.75$, $120° \le \theta \le 180°$, resulting in more than 41 nonequivalent geometries. The constructed PES covers the energies up to $\sim$15 000 cm^{-1} above the minimum of $N_2H^+(\tilde{X}^1\Sigma^+)$. Subsequently, we fitted the calculated energies to the following polynomial expansion, where all points are equally weighted,

TABLE 2: Equilibrium Distances (R_i), Zero Point Vibrational Energy (G_0), Rotational Constants (B_e and D_e), Vibration-Rotation Terms (α_i), Harmonic Wavenumbers (ω_i), Anharmonic Term (g_{22}), *l*-Doubling Constant (q), and Variationally Determined Anahrmonic Wavenumbers (ν_i) of $N_2H^+(\tilde{X}^1\Sigma^+)$ Deduced from the Corresponding 3D-PESs[a]

method	R_{NN}	R_{NH}	G_0	B_e	D_J ($\times 10^5$)	α_1	α_2	α_3	ω_1	ω_2	ω_3	g_{22}	q ($\times 10^3$)	ν_1	ν_2	ν_3
CASSCF/aug-cc-pV6Z	1.0987	1.0388	3497.2	1.5458	0.2829	0.01229	−0.00334	0.01080	3376.4	714.3	2275.7	5.17	7.969	3208.5	697.0	2239.2
MRCI/aug-cc-pV6Z	1.0950	1.0332	3510.5	1.5571	0.2855	0.01251	−0.00352	0.01097	3412.4	704.4	2290.0	5.30	8.133	3238.4	685.7	2252.3
MRCI+Q/aug-cc-pV6Z	1.0957	1.0337	3500.0	1.5552	0.2860	0.01254	−0.00353	0.01102	3407.1	700.0	2283.5	5.30	8.153	3232.8	681.2	2245.6
CCSD/aug-cc-pV5Z	1.0871	1.0319	3589.3	1.5771	0.2760	0.01259	−0.00366	0.01006	3434.4	726.2	2377.4	5.46	8.147	3267.1	708.7	2342.3
CCSD-F12b/aug-cc-pVTZ	1.0874	1.0323	3587.2	1.5762	0.2761	0.01257	−0.00366	0.01007	3431.7	726.4	2375.1	5.46	8.138	3265.0	708.9	2340.1
CCSD(T)/cc-pV5Z	1.0947	1.0339	3510.0	1.5575	0.2840	0.01257	−0.00366	0.01084	3404.1	701.6	2297.6	5.28	8.164	3236.3	685.7	2260.2
CCSD(T)/cc-pV5Z-DK	1.0947	1.0339	3510.2	1.5576	0.2840	0.01257	−0.00366	0.01083	3404.3	701.6	2297.8	5.27	8.165	3236.5	685.7	2260.4
CCSD(T)/aug-cc-pV5Z	1.0947	1.0341	3508.0	1.5573	0.2840	0.01259	−0.00367	0.01084	3401.6	700.9	2297.2	5.27	8.169	3233.9	685.1	2259.7
CCSD(T)/aug-cc-pV6Z	1.0945	1.0341	3508.5	1.5580	0.2841	0.01260	−0.00367	0.01082	3400.6	701.2	2298.3	5.27	8.174	3233.2	685.4	2261.0
CCSD(T)-F12a/aug-cc-pVDZ	1.0963	1.0360	3485.7	1.5527	0.2829	0.01264	−0.00376	0.01090	3391.8	687.5	2291.8	5.15	8.237	3219.7	671.3	2253.8
CCSD(T)-F12a/aug-cc-pVTZ	1.0952	1.0347	3503.2	1.5559	0.2841	0.01259	−0.00366	0.01084	3395.9	700.6	2293.9	5.27	8.161	3228.5	684.6	2256.6
CCSD(T)-F12a/aug-cc-pVQZ	1.0945	1.0343	3508.9	1.5579	0.2839	0.01259	−0.00369	0.01082	3404.1	701.9	2299.0	5.26	8.165	3229.1	684.8	2261.8
CCSD(T)-F12a/aug-cc-pV5Z	1.0942	1.0343	3508.3	1.5586	0.2842	0.01261	−0.00367	0.01082	3398.5	701.5	2299.4	5.27	8.179	3231.4	685.7	2262.1
CCSD(T)-F12b/aug-cc-pVDZ	1.0954	1.0355	3490.8	1.5551	0.2829	0.01264	−0.00377	0.01088	3397.8	687.5	2296.7	5.15	8.257	3225.3	671.0	2258.7
CCSD(T)-F12b/aug-cc-pVTZ	1.0951	1.0345	3505.3	1.5564	0.2840	0.01257	−0.00367	0.01083	3398.8	700.6	2295.2	5.27	8.165	3231.5	684.6	2258.0
CCSD(T)-F12b/aug-cc-pVQZ	1.0944	1.0341	3510.4	1.5581	0.2838	0.01257	−0.00369	0.01081	3406.6	701.9	2299.9	5.26	8.166	3231.4	684.7	2262.6
CCSD(T)-F12b/aug-cc-pV5Z	1.0942	1.0342	3509.3	1.5587	0.2841	0.01261	−0.00367	0.01082	3400.1	701.5	2299.9	5.27	8.180	3232.9	685.6	2262.7
Experiment	1.092698[b]	1.03460[b]	—	1.5539[b]	0.2934[b]	0.01291[c]	−0.003345[c]	0.01100[c]					8.539[c]	3233.952[d]	686.804[c]	2257.867[e]

[a] Distances are in Å and all other values are in cm^{-1}. [b] Reference 14. [c] Reference 10. [d] Reference 11. [e] Reference 12.

TABLE 3: Variationally Computed Rovibrational Spectra of $N_2H^+(\tilde{X}^1\Sigma^+)$ and of its Deuterated Species[a]

N_2H^+ ($\tilde{X}^1\Sigma^+$)						N_2D^+ ($\tilde{X}^1\Sigma^+$)					
σ^+ (J=0)			π (J=1)			σ^+ (J=0)			π (J=1)		
(v_1,v_2,v_3)	Energy	Exp.[b]	(v_1,v_2,v_3)	Energy	Exp.[b]	(v_1,v_2,v_3)	Energy	Exp.	(v_1,v_2,v_3)	Energy	Exp.
(0,0,0)	0.0		(0,1,0)	684.6	688.373*,c	(0,0,0)	0.0		(0,1,0)	543.0	544.568[d]
(0,2,0)	1357.9	1363.337	(0,3,0)	2034.9	2051.359	(0,2,0)	1079.3		(0,3,0)	1616.0	
(0,0,1)	2258.0	2257.873*,c	(0,1,1)	2938.6	2946.617	(0,0,1)	2023.4	2024.0141[e]	(0,1,1)	2569.1	
(0,4,0)	2700.5	2726.230	(0,5,0)	3370.1		(0,4,0)	2146.1		(0,5,0)	2676.8	
(1,0,0)	3231.5	3233.958*,c	(1,1,0)	3892.8	3898.680*,c	(1,0,0)	2634.9	2636.983[f]	(1,1,0)	3158.9	3163.242 [f]
(0,2,1)	3607.9	3621.969	(0,3,1)	4280.6	4310.339	(0,2,1)	3107.8		(0,3,1)	3646.5	
(0,6,0)	4028.4		(0,7,0)	4690.9		(0,6,0)	3201.1		(0,7,0)	3726.2	
(0,0,2)	4492.6	4516.256	(0,1,2)	5168.7	5205.415	(1,2,0)	3676.6		(1,3,0)	4194.6	
(1,2,0)	4543.5	4553.011	(1,3,0)	5197.7	5213.796	(0,0,2)	4026.4		(0,1,2)	4574.4	
(0,4,1)	4941.9		(0,5,1)	5606.9		(0,4,1)	4178.3		(0,5,1)	4710.2	
(0,8,0)	5342.1		(0,9,0)	5997.7		(0,8,0)	4245.2		(0,9,0)	4765.4	
(1,0,1)	5468.0	5469.254*,c	(1,1,1)	6126.0	5935.154	(1,0,1)	4610.8		(1,1,1)	5137.4	
(1,4,0)	5833.1	5864.538	(1,5,0)	6488.0		(1,4,0)	4706.5		(1,5,0)	5219.0	
(0,2,2)	5841.8	5881.165	(0,3,2)	6502.3		(0,2,2)	5115.2		(0,3,2)	5655.8	
(0,6,1)	6260.5		(0,7,1)	6918.0		(2,0,0)	5231.0		(2,1,0)	5736.4	
(2,0,0)	6336.9	6336.679*,c	(2,1,0)	6974.8	6977.265*,c	(0,6,1)	5234.9		(0,7,1)	5759.3	
(0,10,0)	6642.0					(0,10,0)	5280.0		(0,11,0)	5796.5	
(0,0,3)	6703.5	6775.027				(1,2,1)	5657.4		(1,3,1)	6177.5	
(1,2,1)	6773.4	6787.532				(1,6,0)	5725.5				
(1,6,0)	7125.0					(0,0,3)	6008.0				
(0,4,2)	7158.8					(0,4,2)	6189.3				
(2,0,1)	8546.5	8543.163*,c				(0,4,2)	6189.3				

[a] These data are deduced from the CCSD(T)-F12b/aug-cc-pVTZ potential energy surface. All values are in cm^{-1}. [b] Reference 13. *,c * denotes the precise energies as stressed out by Kabbadj et al. [d] Reference 15. [e] Reference 12. [f] Reference 16.

TABLE 4: Variationally Computed Rovibrational Levels of the $\tilde{X}^2\Sigma^+$ Electronic Ground State of N_2H^{++} and its Deuterated Species[a]

N_2H^{++} ($\tilde{X}^2\Sigma^+$)				N_2D^{+2} ($\tilde{X}^2\Sigma^+$)			
σ^+ (J = 0)		π (J = 1)		σ^+ (J = 0)		π (J = 1)	
(v_1,v_2,v_3)	energy	(v_1,v_2,v_3)	energy	(v_1,v_2,v_3)	energy	(v_1,v_2,v_3)	energy
(0,0,0)	0.0[b]	(0,1,0)	535.5	(0,0,0)	0.0[c]	(0,1,0)	429.1
(0,2,0)	1074.1	(0,3,0)	1618.6	(0,2,0)	861.0	(0,3,0)	1295.3
(0,0,1)	1684.1	(0,1,1)	2199.2	(0,0,1)	1302.8	(0,1,1)	1722.6
(0,4,0)	2164.7			(0,4,0)	1731.6	(0,5,0)	2169.9
(1,0,0)	2292.7			(0,2,1)	2144.5		
				(1,0,0)	2247.4		

[a] These data are deduced from our RCCSD(T)-F12b/aug-cc-pVTZ 3D-PES. All values are in cm^{-1}. [b] Used as reference. Zero point vibrational energy $G_0 = 2711.8$ cm^{-1}. [c] Used as reference. Zero point vibrational energy $G_0 = 2335.5$ cm^{-1}.

$$V(R_1,R_2,\theta) = \Sigma_{ijk} c_{ijk} Q_1^i Q_2^j Q_3^k$$

with $Q_u = (R_u - R_u^{ref})/R_u$ for $u = 1$ and 2, and $Q_u = \theta - \theta^{ref}$ for $u = 3$ ($0° \leq \theta \leq 180°$). The index "ref" refers to the reference geometry used during the fit (cf. Table 2). For the fit, we restricted the exponents in the expansion to $i + j + k \leq 4$. For symmetry reasons, we considered only the even values of k. Eventually, in total 22 c_{ijk} coefficients were optimized using a least-squares procedure. The root-mean-square of the fits was less than 5 cm^{-1}.

c. Nuclear Motion Treatment. We derived the 3D-PESs as quartic force fields in internal coordinates. Then, we transformed these force fields, by the l-tensor algebra, to quartic force fields in dimensionless normal coordinates.[33,34] Using second order perturbation theory, we evaluate a set of spectroscopic properties. Moreover, we incorporated our PES expansions in variational calculations using the approach of Carter and Handy.[35] We carried out calculations for $J = 0$ and 1.

III. $N_2H^+(\tilde{X}^1\Sigma^+)$ 3D-Potential Energy Surface and Spectroscopy

In total, we generated 17 3D-PESs for $N_2H^+(\tilde{X}^1\Sigma^+)$ at different levels of theory. We list in Table 2 the spectroscopic data deduced from these 3D-PESs. They include the equilibrium distances, the zero point vibrational energies (G_0), the rotational constants (B_e, D_e and α_i), the anharmonic g_{22} term, the l-doubling constant (q) and the harmonic (ω_i) and the variationally determined anharmonic wavenumbers (ν_i). For comparison, we report in this table the most accurate experimental results. For rotational constants, our data are in close accord with experimental determinations[14] and the recent astrophysical deductions.[7]

When we examine Table 2, one can clearly see that CASSCF, CCSD and CCSD-F12b methods lead to anharmonic wavenumbers (ν_i) differing by ~25 cm^{-1} from the experimental values independently of the quality of the basis set used for the description of N and H atoms. This is signature of the importance of electronic correlation for the good description of the wave function of N_2H^+ $\tilde{X}$. The CCSD(T)-F12/aug-cc-pVDZ method (either a or b approximations) leads to relatively large differences (~15 cm^{-1}). The anharmonic wavenumbers derived from all other calculations are in close agreement with experiment since differences between the measured and computed values are less than 5 cm^{-1}. Especially, the anharmonic wavenumbers deduced using the newly developed CCSD(T)-F12b approximation technique, together with the aug-cc-pVTZ basis set, are in excellent agreement with experimental measure-

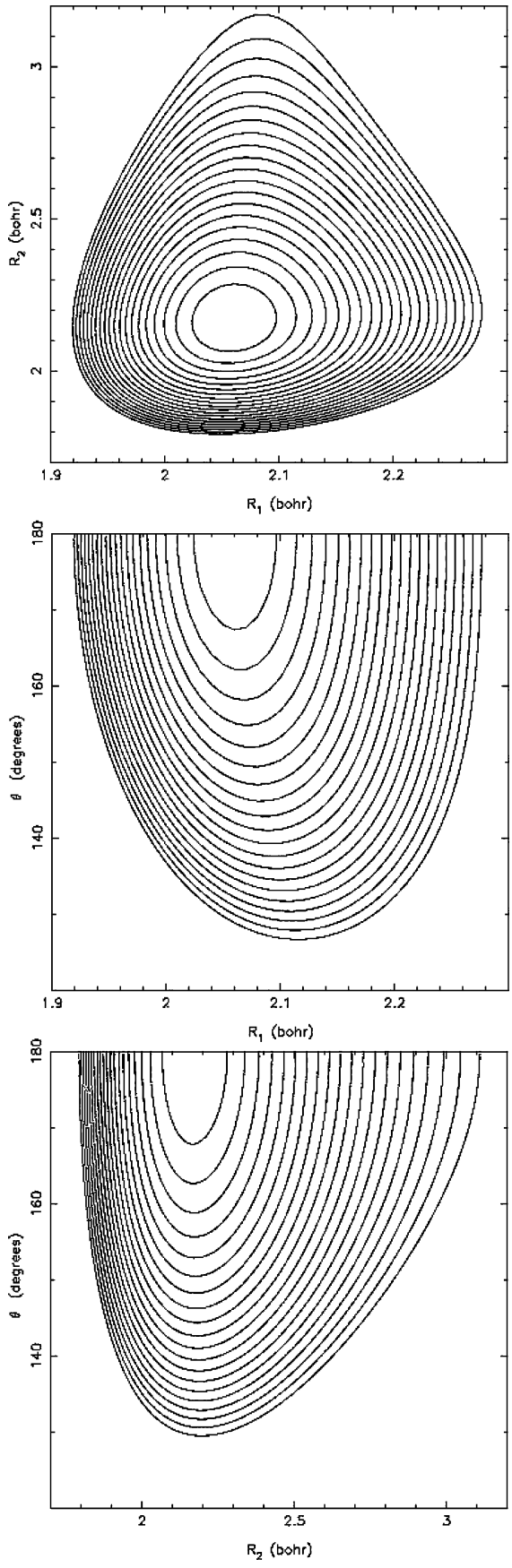

Figure 1. Two dimensional contour plots of the RCCSD(T)-F12b/aug-cc-pVTZ 3D PES of N_2H^{++} ground state along two internal coordinates. The remaining coordinate is set to its equilibrium value (i.e., $R_{e,NN} = 1.0894$ Å, $R_{e,NH} = 1.1473$ Å, $\theta_e = 180°$). The step between the contours is of 250 cm^{-1}.

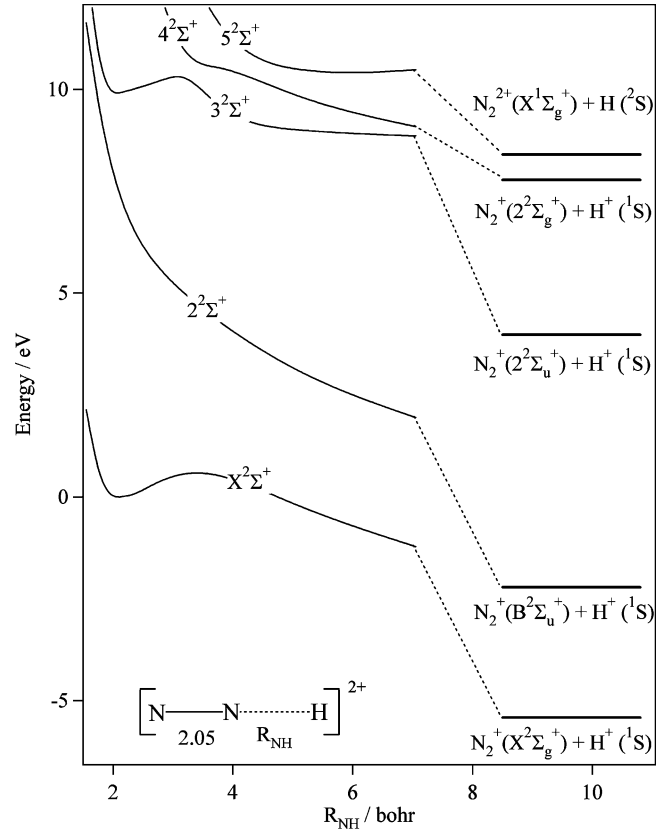

Figure 2. Collinear potential energy curves of the $^2\Sigma^+$ electronic states of N_2H^{++} computed at the MRCI/aug-cc-pV5Z level of theory, along the R_{NH} distance. The R_{NN} distance is kept fixed at 2.05 bohr. These curves are given relative to the $N_2H^{++}(\tilde{X}^2\Sigma^+)$ minimum energy.

ments. These trends are also valid for the other spectroscopic parameters (see Table 2 for more details).

Although similar accuracies are achieved with several *ab initio* methods and basis sets, Table 1 reveals that the cost of these computations varies from 4.66 up to 8594.32 s for a single point calculation. More specifically, the CCSD(T)-F12/aug-cc-pVTZ method is accurate enough with a reduction by 370−40 times of the CPU time needed for such calculations with respect to the MRCI/aug-cc-pV6Z or the CCSD(T)/aug-cc-pV5Z methods, respectively. Hence, CCSD(T)-F12/aug-cc-pVTZ represents a good compromise between cost and accuracy for the generation of full dimensional potential energy surfaces of polyatomic molecules in monoconfigurational electronic states.

As an application of this methodology, we present in Table 3 the full rovibrational spectra of $N_2H^+(\tilde{X}^1\Sigma^+)$ and of $N_2D^+(\tilde{X}^1\Sigma^+)$ up to 7200 and 6200 cm^{-1}, repectively, together with their comparison with the experimental data of refs 12, 13, 15 and 16. For N_2H^+, our computed values differ by less than 6 cm^{-1} from the energies assumed to be precisely determined by Kabbadj et al.[13] (i.e., those denoted by an * in this table). For N_2D^+, similar remarks can be made. However, we notice large discrepancies for some of the N_2H^+ bands, mostly those that are associated with combination modes. For instance, we calculate the (0,2,1) level at 3607.9 cm^{-1} whereas it is measured to be at 3621.969 cm^{-1}. The close lying (1,0,0) fundamental is calculated at less than 3 cm^{-1} from the accurately determined origin. In fact, these bands are weak and are located in a dense region of the IR spectrum, which makes an equivoque assignment and determination of their origins hard as expressed by Kabbadj et al.[13] Further investigations are needed.

IV. N_2H^{++} Ground Potential Energy Surface and Spectroscopy

In a recent study, we prove the existence of the N_2H^{++} dication.[17] The ground electronic state of this dication is of $^2\Sigma^+$ nature. We calculate a potential well of ~0.6 eV before reaching the Coulombic repulsive part of the PES leading to the charge separation fragments. Presently, we mapped the 3D PES of $N_2H^{++}(\tilde{X}^2\Sigma^+)$ close to its equilibrium geometry ($R_{e,NN} = 1.0894$ Å, $R_{e,NH} = 1.1473$ Å, $\theta_e = 180°$). We chose our grid to cover energies below the potential barrier. The electronic calculations are done at the RCCSD(T)-F12b/aug-cc-pVTZ level of theory. Figure 1 displays the two-dimensional cuts of our 3D-PES along two internal coordinates, where we set the others to their equilibrium values. Twenty contours are drawn. The step between the contours is 250 cm^{-1}. Figure 1 shows that both stretchs are coupled together and that the NN (R_1) distance and the in-plane angle (θ) are weakly coupled.

For N_2H^{++} $\tilde{X}$, our calculated spectroscopic parameters, in cm^{-1}, are rotational constants $B_e = 1.5195$ and $D_j = 0.3343 \times 10^{-5}$. The vibration−rotation terms are $\alpha_1 = 0.02526$, $\alpha_2 = -0.00066$ and $\alpha_3 = 0.03087$. The harmonic wavenumbers are computed ω_1 (NN stretching) = 2549.5, ω_2 (bending) = 551.9 and ω_3 (NH stretching) = 1940.0. The *l*-doubling constant and the anharmonic g_{22} term are $q = 0.010$ and $g_{22} = 2.39$, respectively. The variationally determined anharmonic wavenumbers are $\nu_1 = 2292.7$, $\nu_2 = 535.5$ and $\nu_3 = 1684.1$. All of these values represent predictions for $N_2H^{++}\tilde{X}$. Table 4 lists the full rovibrational spectra of N_2H^{++} and N_2D^{+2} up to 2300 cm^{-1} above the zero point vibrational energy. The isotopic shifts are calculated to be $\Delta\nu_1 = 45.3$, $\Delta\nu_2 = 106.4$, $\Delta\nu_3 = 381.3$. We notice a strong reduction of ν_2 and ν_3. However, the sensitive ν_1 decrease is because of the couplings between the R_1 and the other internal coordinates mentioned above. In contrast to the singly charged ion, no anharmonic resonances are located in the low energy part of the rovibrational spectra of this dication.[9]

V. Implications for Titan's Atmosphere

In the atmosphere of Titan, we expect the formation of N_2H^{++} by electron impact ionization or VUV double photoionization of the neutral N_2H molecule. This dication should also be an intermediate or a product of ion−molecule reactions taking place there. Reactive collisions between N_2^+ with H^+, H_2^+ or ionized hydrocarbons[2] should produce this dication. Moreover, we may form N_2H^{++} after reactive collisions between N_2^{++} and H or H_2 or the Titan's hydrocarbons. For illustration, Figure 2 shows that collisions between N_2^{++} and H lead to the population of the shallow minimum of $N_2H^{++}(5^2\Sigma^+)$. Then, the N_2H^{++} ground state is reached at least after internal conversion through the avoided crossings between the $^2\Sigma^+$ states. N_2H^{++} $\tilde{X}$ may be produced after reaction between $N_2^+ + H^+$, when they possess enough energy to overcome the potential barrier (of 6 eV) computed for the $\tilde{X}^2\Sigma^+$ electronic ground state (cf. Figure 2).

Our prediction of a metastable N_2H^{++} dication is not without consequences on the ionic chemistry where the N_2H^+ ion is present, especially for the ionosphere of Titan. Recently, Lilensten et al.[36] definitely predicted the existence of a N_2^{++} layer in the upper atmosphere of Titan. The reactions involving this species and forming N_2H^{++} are omitted in the models dedicated for the study of the gas phase chemistry occurring there. Our data should be incorporated in these models and should help in the identification of the N_2H^{++} dication in these media.

VI. Conclusion

The (R)CCSD(T)-F12 approach represents a low cost and accurate enough technique for the generation of the multidimensional potential energy surfaces of atmospherical and astrophysical relevant systems dominantly described by a unique electron configuration. The rovibrational spectra deduced from these PESs compare well to the most accurate experimental determinations. For electronic states described by a multi configurational wave function and for electronic excited states studies, we should still use the CASSCF and MRCI more expensive methods. This benchmark study opens new perspective for the investigation of other important molecules or bimolecular reactive or nonreactive de-excitation phenomena relevant for planetary and astrophysical media.

References and Notes

(1) Fox, J. L.; Yelle, R. V. NASA-CR-200657, 1996 and references therein.
(2) Vuitton, V.; Yelle, R. V.; McEwan, M. J. *Icarus* **2007**, *191*, 722.
(3) Daniel, F.; Dubernet, M.-L.; Meuwly, M. *J. Chem. Phys.* **2004**, *121*, 4540.
(4) Daniel, F.; Cernicharo, J.; Dubernet, M.-L. *ApJ* **2006**, *648*, 461.
(5) Daniel, F.; Cernicharo, J.; Roueff, E.; Gerin, M.; Dubernet, M.-L. *ApJ* **2007**, *667*, 980.
(6) Emprechtinger, M.; Caselli, P.; Volgenau, N. H.; Stutzki, J.; Wiedner, M. C. *A.&A.* **2009**, *493*, 89.
(7) Pagani, L.; Daniel, F.; Dubernet, M.-L. *A.&A.* **2009**, *494*, 719.
(8) Dore, L.; Bizzocchi, L.; Degli Esposti, C.; Tinti, F. *A.&A.* **2009**, *496*, 275.
(9) Špirko, V.; Bludský, O.; Kraemer, W. P. *Collect. Czech. Chem. Commun.* **2008**, *73*, 873.
(10) Owrutsky, J. C.; Gudeman, C. S.; Martner, C. C.; Tack, L. M.; Rosenbaum, N. H.; Saykally, R. J. *J. Chem. Phys.* **1986**, *84*, 605.
(11) Keim, E. R.; Polak, M. L.; Owrutsky, J. C.; Coe, J. V.; Saykally, R. V. *J. Chem. Phys.* **1990**, *93*, 3111, and references therein.
(12) Foster, S. C.; McKellar, A. R. W. *J. Chem. Phys.* **1984**, *81*, 3424.
(13) Kabbadj, Y.; Huet, T. R.; Gabrys, C. M.; Oka, T. *J. Mol. Spectrosc.* **1994**, *163*, 180.
(14) Amano, T.; Hirao, T.; Takano, J. *J. Mol. Spectrosc.* **2005**, *234*, 170.
(15) Sears, T. J. *J. Chem. Phys.* **1985**, *82*, 5757.
(16) Nesbitt, D. J.; Petek, H.; Gudeman, C. S.; Moore, C. B.; Saykally, R. J. *J. Chem. Phys.* **1984**, *81*, 5281.
(17) Brites, V.; Hochlaf, M. *Chem. Phys. Lett.* 2009. submitted.
(18) Knowles, P. J.; Werner, H.-J. *Chem. Phys. Lett.* **1985**, *115*, 259.
(19) Werner, H.-J.; Knowles, P. J. *J. Chem. Phys.* **1988**, *89*, 5803.
(20) Knowles, P. J.; Werner, H.-J. *Chem. Phys. Lett.* **1988**, *145*, 514.
(21) Langhoff, S. R.; Davidson, E. R. *Int. J. Quantum Chem.* **1974**, *8*, 61.
(22) Knowles, P. J.; Hampel, C.; Werner, H.-J. *J. Chem. Phys.* **1993**, *99*, 5219; Erratum: *J. Chem. Phys.* **2000**, *212*, 3106.
(23) http://www.molpro.net.
(24) Werner, H. J.; Adler, T. B.; Manby, F. R. *J. Chem. Phys.* **2007**, *126*, 164102.
(25) Adler, T. B.; Knizia, G.; Werner, H.-J. *J. Chem. Phys.* **2007**, *127*, 221106.
(26) Peterson, A. K.; Adler, Y. B.; Werner, H.-J. *J. Chem. Phys.* **2008**, *128*, 084102.
(27) Dunning, T. H., Jr. *J. Chem. Phys.* **1989**, *90*, 1007.
(28) Wilson, A. K.; Mourik, T. V.; Dunning, T. H., Jr. *J. Mol. Struct.* **1997**, *388*, 339.
(29) Dunning, T. H., Jr.; Peterson, K. A.; Wilson, A. K. *J. Chem. Phys.* **2001**, *114*, 9244.
(30) Weigend, F. *Phys. Chem. Chem. Phys.* **2002**, *4*, 4285.
(31) Hättig, C. *Phts. Chem. Chem. Phys.* **2005**, *7*, 59.
(32) Klopper, W. *Mol. Phys.* **2001**, *99*, 481.
(33) Senekowitsch, J. Thesis of the University of Frankfurt, Germany (1988).
(34) Mills in, I. M. *Molecular Spectroscopy: Modern Research*; Rao, K. N., Mathews, C. W., Eds.; Academic Press: New York, 1972.
(35) Carter, S.; Handy, N. C. *Comput. Phys. Rev.* **1987**, *5*, 117.
(36) Lilensten, J.; Witasse, O.; Simon, C.; Soldi-Lose, H.; Dutuit, O.; Thissen, R.; Alcaraz, C. *Geophys. Res. Lett.* **2005**, *32*, L03203.

JP903701X